Gap states in Pentacene Thin Film Induced by Inert Gas Exposure

Fabio Bussolotti,[1,*] Satoshi Kera,[1] Kazuhiro Kudo,[2] Antoine Kahn,[3] and Nobuo Ueno[1,†]

[1]*Department of Nanomaterial Science, Graduate School of Advanced Integration Science, Chiba University, Chiba 263-8522, Japan*
[2]*Department of Electrical and Electronics Engineering, Graduate School of Engineering, Chiba University, Chiba 263-8522, Japan*
[3]*Department of Electrical Engineering, Princeton University, Princeton, New Jersey 08544, USA*

(Received 13 February 2013; published 25 June 2013)

We studied gas-exposure effects on pentacene (Pn) films on SiO_2 and Au(111) substrates by ultrahigh sensitivity photoelectron spectroscopy, which can detect the density of states of $\sim 10^{16}$ states $eV^{-1}\,cm^{-3}$ comparable to electrical measurements. The results show the striking effects for Pn/SiO_2: exposure to inert gas (N_2 and Ar) produces a sharp rise in gap states from $\sim 10^{16}$ to $\sim 10^{18}$ states $eV^{-1}\,cm^{-3}$ and pushes the Fermi level closer to the valence band (0.15–0.17 eV), as does exposure to O_2 (0.20 eV), while no such gas-exposure effect is observed for Pn/Au(111). The results demonstrate that these gap states originate from small imperfections in the Pn packing structure, which are induced by gas penetration into the film through the crystal grain boundaries.

DOI: 10.1103/PhysRevLett.110.267602 PACS numbers: 79.60.Fr, 71.20.Rv, 79.60.Dp, 81.05.Fb

The energy level alignment (ELA) at organic-substrate and organic-organic interfaces is a crucial issue for any organic-based device, given that the interface electronic structure controls the charge injection process in the organic semiconductor (OSC) [1,2]. Despite considerable effort [1–5], however, it still remains a mystery why some organic semiconductors, such as pentacene, always show *p*-type charge transport property while some others, such as C_{60}, show *n*-type property without heavy intentional doping; that is, the transport property seems to be determined by molecule itself. Therefore, a consensus on the ELA mechanism has yet to be reached.

Recently, the ELA mechanism was suggested to originate with the density of gap states (DOGS) caused by structural disorder in the intermolecular packing [1,4,6–8]. Such gap states also introduce electronic traps in the bulk of OSCs, which limit the electron or hole transport in the material [9,10]. Moreover, exposure of OSC films to various gaseous atmospheres was reported to affect the ELA and the charge transport properties [11–14]. In general, such effects were discussed in terms of chemical reactions between gas molecules and organic molecules [11–14]. However, in addition to *chemical* effects, the simple penetration of gas molecules in organic solids may alter the intermolecular packing structure [15,16]. This more *physical* alteration can also modify the electronic properties of the organic films because (i) the gas penetration could induce changes in the intermolecular packing structure, thus resulting in gap states [17,18] and (ii) the valence band structure of organic solids is strongly dependent on the intermolecular packing geometry due to planar molecular structure [19].

In this work, we report a direct study of the energy distribution of DOGS of the order of 10^{16} states $eV^{-1}\,cm^{-3}$, which is comparable to DOGS detected by electrical measurements [9], in an organic layer by means of the ultralow background, high sensitivity ultraviolet photoemission spectroscopy (UPS) technique. We investigate pentacene (Pn), an OSC that is widely used in organic field effect transistors [20], deposited on $SiO_2/Si(100)$ and Au(111) substrates at RT. The impact of exposure to 1-atm of inert N_2 atmosphere on the Pn electronic properties is evaluated. Despite the absence of chemical interaction between N_2 and Pn molecules, the DOGS and ELA at the Pn/SiO_2 interface are strongly modified by the exposure to N_2 gas. This effect is ascribed to the structural disorder caused by N_2 molecules penetrating into the Pn film. A similar effect is observed upon exposure to Ar, while in the case of O_2 exposure, the DOGS formation is accelerated, presumably because of the difference in the chemical properties of the gas molecules.

The present results demonstrate that structural disorder has a significant impact on the electronic properties and interfacial ELA in organic thin films. This is related to the nature of organic semiconductor crystals, which consists of low-symmetry molecules held together by weak intermolecular forces. The results also have great practical significance, as they show that organic layer processing in an inert atmosphere (N_2), which is ubiquitous in organic electronics, does affect the electronic structure of the OSC, a point which had not been understood so far.

Si(100) wafers (*n*-type) with a thermally grown SiO_2 layer (thickness = 3 nm) were cleaned in an acetone and an isopropanol ultrasonic bath. The SiO_2 substrates were then annealed in a UHV preparation chamber ($\sim 4 \times 10^{-8}$ Pa) at 673 K for 12 h. Pn molecules ($C_{22}H_{14}$, Sigma Aldrich), purified by three cycles of vacuum sublimation, were vacuum deposited onto the SiO_2 substrate at room temperature (293 K, RT). The deposition rate (0.5 nm/min) was monitored by using a quartz microbalance. During the Pn deposition, the pressure was stably

maintained below 6×10^{-8} Pa. As-deposited Pn thin films were reported to have an upright-standing molecular orientation and herringbonelike intermolecular packing, as judged from the HeI_α UPS spectral profile [19,21]. The Pn thin films were repeatedly exposed to 1-atm N_2 with a purity of 99.99995% (6N5) at RT (293 K) for a total exposure time of 20 h. Next, the film was exposed to 1-atm O_2 (6N5) for an additional 5 h at RT. This gas exposure procedure was repeated using Ar gas (5N5) on different samples. The effect of the N_2 exposure on Pn thin film on a clean Au(111) single crystal surface (thickness = 40 nm, RT deposition) was also evaluated. The gas exposures were performed by using a UHV-compatible gas inlet line connected to the preparation chamber.

The UPS measurements were performed at RT using an ultrahigh-sensitivity UPS apparatus with a hemispherical electron energy analyzer (MBS A-1) and a monochromatic XeI_α ($h\nu = 8.437$ eV) radiation source with a LiF single crystal filter. The electrical wiring of the measurement system was carefully performed to minimize the background noises by positioning the electrical cables at appropriate positions. The accumulation time of the spectra was typically 40 min. Under these conditions, radiation damage effects [22] to the Pn films could be excluded (See Sec. I of the Supplemental Material [23]). All UPS spectra were measured at normal emission with an acceptance angle of $\pm 18°$, and a bias of -5 V was applied to the sample in order to measure the vacuum level (VL) (see Sec. II the Supplemental Material [23]). The energy resolution of the UPS system was set to 30 meV. The binding energy scale was relative to the substrate Fermi level.

Figure 1(a) shows the XeI_α-UPS spectra of the as-deposited and N_2- (O_2-) exposed Pn film (15 nm) in the cutoff and highest occupied molecular orbital (HOMO) regions [spectra (1)–(7)]. The HOMO band of the as-deposited Pn thin film consists of two main components [labeled H_1 and H_2 in Fig. 1(a)] with an energy separation of ~0.45 eV. The two components correspond to the density of states (DOS) of the HOMO band in Pn thin film with an upright-standing molecular orientation and herringbone-like intermolecular packing [21,24]. The H_1 (H_2) position was determined by a least-squares fitting of the HOMO-band UPS data using Gaussian functions (see Sec. III of the Supplemental Material [23]). Following each N_2 exposure, the H_1 (H_2) peak shifts towards low binding energies, while the vacuum level (VL) moves upwards by

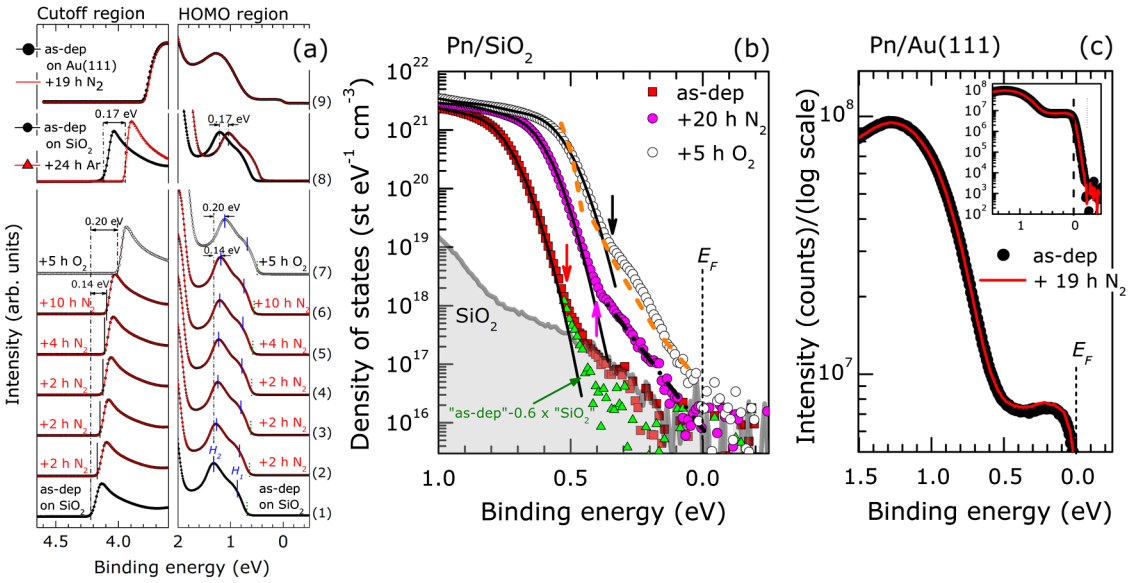

FIG. 1 (color online). (a) XeI_α-UPS spectra of as-deposited [spectrum (1)], N_2-exposed [spectra (2)–(6)], O_2-exposed [spectra (7)] and Ar-exposed [spectra (8)] Pn thin film (15 nm) on SiO_2 substrate. Spectrum (9) includes the UPS data of as-deposited and N_2-exposed Pn/Au(111) thin film (40 nm) acquired at RT. The positions of the VL and HOMO derived bands (H_1 and H_2) are indicated by vertical (continuous) bars. The difference between the VL (HOMO) positions of the Pn/SiO_2 thin films in the "N_2" and "Ar" experiments reflects the difference between the initial SiO_2 work functions. (b) DOS (log scale intensity plot) of as-deposited [closed (red) square symbols], N_2-exposed [20 h, closed (magenta) circles] and O_2-exposed (5 h, open circles) Pn thin film on SiO_2. Continuous (black) lines are the cumulative fitting curve of the HOMO band (see Sec. III of the Supplemental Material [23]). DOS values were extracted from the UPS data, as described in Ref. [24]. SiO_2 data are rescaled to preserve, in the DOS scale, their relative intensity with respect to the as-deposited Pn data. Vertical arrows indicate the threshold energy position (E_T) where the DOS distribution deviates from the cumulative fitting curve and DOGS starts to appear. The dashed line indicates the DOGS of the Pn thin film as determined by transport measurements. Data are adapted from Ref. [12]. (c) XeI_α-UPS spectra of as-deposited Pn thin film on Au(111) (40 nm) before and after N_2 exposure. The Fermi edge of the Au(111) substrate is clearly visible (see also inset). No spectral change was detected upon gas exposure.

the same amount. This N_2-induced "rigid" energy shift almost saturates after a total exposure time of 20 h. Further exposure to O_2 (5 h) produces an additional energy shift [spectra (7)]. Interestingly, the ionization potential (IP) of the as-deposited Pn thin film ($IP = 4.90$ eV) is unchanged upon the various gas exposure treatments. The IP of an organic thin film was reported to be strongly dependent on the molecular orientation [25] and molecular packing [21]. Therefore, the stability of the IP in the present case indicates that no large-scale structural rearrangement occurs. Similar results are obtained for the Ar-exposed Pn/SiO_2 thin film [spectra (8)], while no spectral shift is detected for Pn/Au(111) thin film after prolonged exposure (19 h) to 1-atm N_2 [spectra (9)].

Figure 1(b) shows the expanded UPS spectra of the HOMO and gap energy region on log scale for the as-deposited, N_2-exposed (total exposure time = 20 h) and O_2-exposed (total exposure time = 5 h following the 20 h N_2 exposure) Pn thin film with the corresponding fitting curves (see Sec. III of the Supplemental Material [23]). The UPS spectrum of the SiO_2 substrate is shown for comparison. The DOGS of the as-deposited Pn film is very low, but it significantly increases after N_2- and O_2-exposure (the progressive increase in DOGS with gas exposure time is shown in Sec. IV of the Supplemental Material [23]). Ar-exposure leads to a similar DOGS increase (not shown). In the gap state binding energy region ($\sim$ 0–0.5 eV), the DOS of the as-deposited Pn film and the SiO_2 substrate are comparable [Fig. 1(b)]. Therefore, the SiO_2 DOS may overlap with the DOGS of the as-deposited Pn film in a way that depends on the electron mean free path in the Pn overlayer (see Sec. V of the Supplemental Material [23]). Once the substrate contribution is taken into account, the DOGS of the as-deposited film ($\sim 10^{16}$ states $eV^{-1}\,cm^{-3}$) turns out to be comparable to that detected by electrical measurements for Pn on SiO_2 [9,12]. For the gas-exposed Pn films, the DOGS is $\sim$10 times larger than the contribution from the substrate, and can therefore be unambiguously related to the Pn film. In particular, for the N_2-exposed sample, an exponential-type DOGS [linear on the log scale of Fig. 1(b)] is clearly visible between the HOMO threshold energy $E_T = 0.4$ eV (where the DOS starts deviating from a Gaussian line shape) and the Fermi level (E_F). A different energy dependence is observed for the DOGS of the O_2-exposed sample. Postannealing experiments (50 °C for 18 h) on N_2-exposed Pn films show a gradual recovery to the original VL and HOMO positions (i.e., before gas exposure). At the same time, a decrease in the DOGS is observed (see Sec. VI of the Supplemental Material [23]). Consequently, the DOGS of the gas-exposed sample can be ascribed to a slight intermolecular packing disorder resulting from prolonged gas exposure. These gap states may in turn affect the position of E_F within the energy gap [7]. A similar effect was observed for thinner Pn films (not shown). Note that no residual N_2 is detected by x-ray photoemission spectroscopy in the gas-exposed film following reintroduction into UHV (see Sec. VII of the Supplemental Material [23]). This supports the conclusion that the DOGS is not due to N_2-related states but rather to intermolecular packing disorder. The increase in DOGS and its different energy distribution upon O_2 exposure can probably be ascribed to (i) a more effective penetration of O_2 molecules into the Pn film (the penetration of a gas into organic systems strongly depends on its chemical properties and size [16]) and/or (ii) chemical interaction between O_2 molecules and Pn molecules [11,26]. However, it is worth noting that a prolonged N_2 exposure of Pn films prepared at RT on single crystalline Au(111) does not induce any detectable change in the DOGS or spectral shift [Figs. 1(a) and 1(c)]. Pn films deposited on Au(111) was reported to exhibit larger crystallites [size $\sim$ 200 nm] and significantly fewer grain boundaries than those on SiO_2 [27,28], suggesting that grain boundaries play a crucial role in the penetration of gas molecules and in the changes of the intermolecular packing geometry as depicted in Fig. 2. According to the UPS data [Fig. 1(b)], the defect density is estimated to be in the range of 10^{16}–10^{18} cm^{-3}, corresponding to a defect-to-molecule ratio of 10^{-5}–10^{-3}, which is hardly detectable via structural diffraction

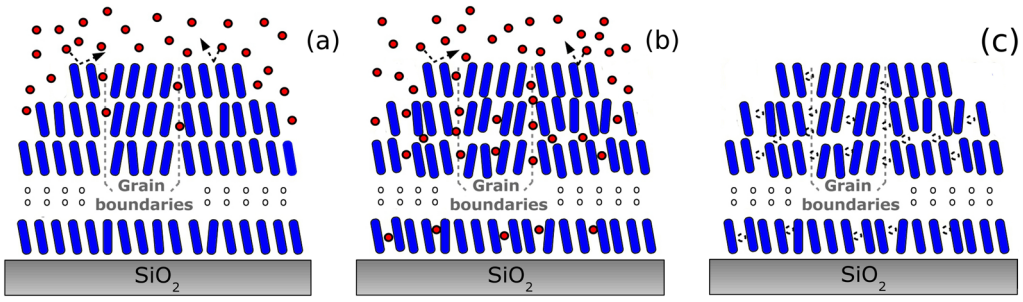

FIG. 2 (color online). Schematic representation of the gas penetration and mediated imperfections in Pn thin film on SiO_2. During exposure [panel (a)], gas molecules progressively penetrate into the Pn film, where they *locally alter* the original intermolecular packing geometry [panel (b)]. The gas penetration proceeds through the grain boundaries of the film. Because of the weak N_2-Pn interaction, N_2 molecules are easily removed once the film is put back in UHV. The result is a weakly disordered film [(panel (c)].

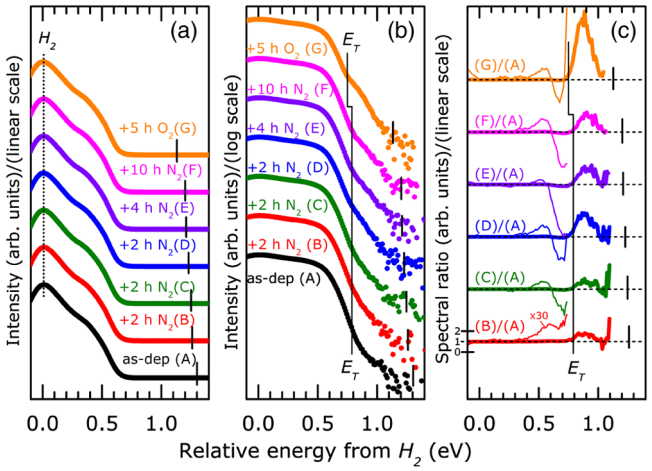

FIG. 3 (color online). (a) XeI$_\alpha$-UPS data of as-deposited, N_2-exposed and O_2-exposed Pn/SiO_2 thin film in the HOMO band region. The energy scale is referred to the H_2 position (dotted line) where the HOMO band reaches the maximum intensity. The vertical, short bars on each plot indicate the position of the Fermi level. The SiO_2 substrate signal was not removed from the as-deposited sample spectra. (b) Same as panel (a), but plotted on a log scale. The continuous (black) line indicates the position of the threshold energy (E_T) from which the gap state energy distribution starts to appear. (c) Spectral ratio between the data of gas-exposed film and as-deposited film (see text for details).

techniques [29]. The hypothesis that the DOGS is mediated by structural defects in the Pn film is also supported by theoretical calculations by Kang *et al.* [17]. They showed that (i) sliding defects along the Pn long axis create shallow gap states and (ii) the HOMO levels at the defect sites are distributed over a range of up to 100 meV from the HOMO of the unperturbed molecules.

According to this model, the DOS in the HOMO (gap state) binding energy region is expected to decrease (increase) with the density of defects. To verify this point, the evolution of the UPS intensity upon gas exposure is carefully evaluated. First, the XeI$_\alpha$-UPS spectra of as-deposited, N_2-exposed and O_2-exposed Pn thin films are aligned to the position of the HOMO band maximum (H_2) [Figs. 3(a) and 3(b)]. Next the ratio between the UPS spectra of the gas-exposed and the as-deposited samples is evaluated for each gas-exposure step [Fig. 3(c)]. For long exposure times (≥ 2 h), the increase in the UPS intensity in the gap state energy region (spectral ratio > 1, $E > E_T$) corresponds to a reduction in the HOMO band intensity (spectral ratio < 1) within $\sim$0.2 eV from the threshold position. This result is in qualitative agreement with the theoretical prediction [17]. In the high intensity region of the HOMO band (~ 0.5 eV) the slight increase of the electronic states and/or the small broadening in the HOMO line shape, as due to structural disorder induced by gas exposure [18], results in the slight increase of the spectral ratio (observed at $\sim$0.5 eV).

Finally, we comment on the impact of the gas exposure on the observed molecular level shift, i.e., the shift of the HOMO level towards E_F (see Fig. 1(a) and also Sec. VIII of the Supplemental Material [23]). We suggest that the lowest unoccupied molecular orbital (LUMO) of Pn also gives rise to a distribution of (unoccupied) gap states resulting from imperfections in the intermolecular packing [17]. The energy distributions of the HOMO- and LUMO-derived DOGS are not symmetric because the corresponding wave functions have different spatial spreads [17]. Such disorder-induced nonsymmetric DOGS (tailing states) affect the position of E_F within the gap of organic semiconductors. Depending on the DOGS and their energy distribution, E_F may lie closer to the pristine LUMO or HOMO band [18]. With increasing structural disorder (as induced, for example, by gas exposure) E_F is expected to lie even closer to the HOMO, as observed in the present work (see Fig. 1(a) and Sec. VIII of the Supplemental Material [23]).

In conclusion, ultralow background, high-sensitivity UPS allowed us to directly measure the DOGS in pristine Pn thin films grown on SiO_2 and to determine values of the order of 10^{16} states $eV^{-1}\,cm^{-3}$, comparable to those obtained by electrical measurements. Striking effects due to gas exposure are that (i) exposure to 1-atm of inert gas (N_2 or Ar) produces a rise in gap state density, as does exposure to O_2, (ii) these gap states push the Fermi level closer to the HOMO, and (iii) the gap states originate from small imperfections in the Pn packing structure induced by gas molecule penetration into the film, presumably through the crystal-grain boundaries. Such imperfections remain even after removal of the gas molecules to yield gap states that are responsible to control the E_F position within the gap. The present findings demonstrate the significant impact of slight structural disordering on the electronic properties of organic thin films. Furthermore, they reveal that complete control of the organic film structure is a requisite for producing organic devices with the desired properties. Finally, they clearly demonstrate that, contrary to a widely held assumption, processing of organic films such as Pn in inert atmosphere is not without negative impact on the electronic structure of the material.

The authors acknowledge the support from the G-COE program at Chiba University (G-03, MEXT), Grant-in Aid for Scientific Research [(A) JSPS Grant No. 24245034 and (B) JSPS Grants No. 23360005 and No. 23360006]. Work at Princeton was supported by the National Science Foundation (Grant No. DMR-1005892).

*Corresponding author.
fabio@restaff.chiba-u.jp
†Corresponding author.
uenon@faculty.chiba-u.jp

[1] J. Hwang, E. J. Kim, J. Liu, J. L. Bredas, A. Duggal, and A. Kahn, J. Phys. Chem. C **111**, 1378 (2007).

[2] G. Heimel *et al.*, Nat. Chem. **5**, 187 (2013).
[3] S. Kera, Y. Yabuuchi, H. Yamane, H. Setoyama, K. K. Okudaira, A. Kahn, and N. Ueno, Phys. Rev. B **70**, 085304 (2004).
[4] H. Y. Mao, F. Bussolotti, D.-C. Qi, R. Wang, S. Kera, N. Ueno, A. T. S. Wee, and W. Chen, Org. Electron. **12**, 534 (2011).
[5] M. Fahlman, A. Crispin, X. Crispin, S. K. M. Henze, M. P. de Jong, W. Osikowicz, C. Tengstedt, and W. R. Salaneck, J. Phys. Condens. Matter **19**, 183202 (2007).
[6] H. Fukagawa, S. Kera, T. Kataoka, S. Hosoumi, Y. Watanabe, K. Kudo, and N. Ueno, Adv. Mater. **19**, 665 (2007).
[7] T. Sueyoshi, H. Fukagawa, M. Ono, S. Kera, and N. Ueno, Appl. Phys. Lett. **95**, 183303 (2009).
[8] S. Yogev, R. Matsubara, M. Nakamura, U. Zschieschang, H. Klauk, and Y. Rosenwaks, Phys. Rev. Lett. **110**, 036803 (2013).
[9] W. L. Kalb, S. Haas, C. Krellner, T. Mathis, and B. Batlogg, Phys. Rev. B **81**, 155315 (2010).
[10] S. Olthof, S. Mehraeen, S. K. Mohapatra, S. Barlow, V. Coropceanu, J.-L. Brédas, S. R. Marder, and A. Kahn, Phys. Rev. Lett. **109**, 176601 (2012).
[11] D. V. Lang, X. Chi, T. Siegrist, A. M. Sergent, and A. P. Ramirez, Phys. Rev. Lett. **93**, 086802 (2004).
[12] F. De Angelis, S. Cipolloni, L. Mariucci, and G. Fortunato, Appl. Phys. Lett. **88**, 193508 (2006).
[13] G. Gu and M. G. Kane, Appl. Phys. Lett. **92**, 053305 (2008).
[14] T. Nishi, K. Kanai, Y. Ouchi, M. R. Willis, and K. Seki, Chem. Phys. Lett. **414**, 479 (2005).
[15] A. Kondo, H. Noguchi, S. Ohnishi, H. Kajiro, A. Tohdoh, Y. Hattori, W.-C. Xu, H. Tanaka, H. Kanoh, and K. Kaneko, Nano Lett. **6**, 2581 (2006).
[16] H. Kajiro, A. Kondo, K. Kaneko, and H. Kanoh, Int. J. Mol. Sci. **11**, 3803 (2010).
[17] J. H. Kang, D. Da Silva Filho, J.-L. Bredas, and X. Y. Zhu, Appl. Phys. Lett. **86**, 152115 (2005).
[18] T. Sueyoshi, H. Kakuta, M. Ono, K. Sakamoto, S. Kera, and N. Ueno, Appl. Phys. Lett. **96**, 093303 (2010).
[19] H. Yoshida and N. Sato, Phys. Rev. B **77**, 235205 (2008).
[20] M. Kitamura and Y. Arakawa, J. Phys. Condens. Matter **20**, 184011 (2008).
[21] H. Fukagawa, H. Yamane, T. Kataoka, S. Kera, M. Nakamura, K. Kudo, and N. Ueno, Phys. Rev. B **73**, 245310 (2006).
[22] B. Boudaïffa, P. Cloutier, D. Hunting, M. A. Huels, and L. Sanche, Science **287**, 1658 (2000).
[23] See Supplemental Material at http://link.aps.org/supplemental/10.1103/PhysRevLett.110.267602 for details about data analysis, irradiation effects, annealing treatments and XPS results.
[24] F. Bussolotti, S. Kera, and N. Ueno, Phys. Rev. B **86**, 155120 (2012).
[25] S. Duhm, G. Heimel, I. Salzmann, H. Glowatzki, R. L. Johnson, A. Vollmer, J. P. Rabe, and N. Koch, Nat. Mater. **7**, 326 (2008).
[26] I. Salzmann, S. Duhm, R. Opitz, J. P. Rabe, and N. Koch, Appl. Phys. Lett. **91**, 051919 (2007).
[27] D. Käfer, C. Wöll, and G. Witte, Appl. Phys. A **95**, 273 (2009).
[28] D. Käfer, L. Ruppel, and G. Witte, Phys. Rev. B **75**, 085309 (2007).
[29] T. Hosokai, A. Hinderhofer, A. Vorobiev, C. Lorch, T. Watanabe, T. Koganezawa, A. Gerlach, N. Yoshimoto, Y. Kubozono, and F. Schreiber, Chem. Phys. Lett. **544**, 34 (2012).